Original Article

In-vitro Characterization and Evaluation of *Beta Vulgaris* L. Extract Loaded on Chitosan Nanoparticles as Anticandidal and Antibiofilm Activity

Zahraa A. Al-Ameri[1*], Muna T. Al-Musawi[2], Lbeeb Ahmed Alzubaidi[3]

1. Department of Medical Laboratory Techniques, Al-Farahidi University, Baghdad, Iraq.
2. Department of Biology, College of Science for Women, University of Baghdad, Baghdad, Iraq.
3. Environmental and Water Directorate, Ministry of Science and Technology, Baghdad, Iraq.

Use your device to scan and read the article online

How to Cite This Article Al-Ameri, Z. A., Al-Musawi, M. T., & Alzubaidi, L, A. (2024). In-vitro Characterization and Evaluation of Beta Vulgaris L. Extract Loaded on Chitosan Nanoparticles as Anticandidal and Antibiofilm Activity. *Iranian Journal of Veterinary Medicine, 18*(4), 649-660. http://dx.doi.org/10.32598/ijvm.18.specialissue.11

http://dx.doi.org/10.32598/ijvm.18.specialissue.11

ABSTRACT

Background: The most common *Candida* species, *Candida albicans*, is one of more than 20 species that may cause candidiasis, an infection that can manifest as a systemic, deep, or superficial, infection. Due to their ability to produce several mechanisms to survive, *Candida* spp. needed a novel approach to fight them. In this context, nanotechnology is presented as an effective technique used to treat such pathogens.

Objectives: This study investigates the preparation of the green synthesis of nanoparticles (NPs), using red beetroot (*Beta vulgaris* L. extract [BVE]) loaded on chitosan and the estimation of their anticandidal and antibiofilm activity against drug-resistant *Candida* species. This novel strategy possibly addresses the problems caused by Candida species, such as antibiotic resistance and biofilm development, using the synergistic antibacterial qualities of plant extract and the biocompatible nature nanoparticles

Methods: Extremely drug-resistant *Candida* spp. (*C. parapsilosis, C. glabrata, C. lusitaniae*, and *C. auris*) were isolated from clinical specimens and identified using the CHROMagar *Candida* culture medium, Vitek-2 system, and molecular diagnosis, then prepared BVE and biosynthesis of chitosan NPs (chitosan NPs loaded BVE) and we studied their characterization (morphological and structural aspects) by ultraviolet-visible absorption spectroscopy, atomic force microscopy, scanning electron microscopy, x-ray diffraction (XRD), energy dispersive x-ray, and high-performance liquid chromatography followed by the estimation of its minimum inhibitory concentration and sub-minimum inhibitory concentration and anti-biofilm activity.

Results: The extreme drug resistance patterns showed the chitosan NPs loaded BVE peak of 2θ value at 22.86 ˚C and an intensity level at 736.55 counts. Atomic force microscopy images found that the particle size ranged from 26.74 to 53.96 nm. Meanwhile, the morphology of chitosan NPs loaded BVE was investigated using scanning electron microscopy which had a spherical appearance with a diameter range of 37.99-56.28 nm. The energy-dispersive x-ray

Article info:
Accepted: 17 Oct 2023
Publish: 01 Oct 2024

*** Corresponding Author:**
Zahraa Abbas Al-Ameri
Address: *Department of Medical Laboratory Techniques, Al-Farahidi University, Baghdad, Iraq.*
Phone: *+964 (772) 8667003*
E-mail: *zahraali1471997@gmail.com*

examination revealed a significant signal at 1.5 keV and 2.3 keV. The high-performance liquid chromatography analysis showed the existence of flavonoids but no lysine and vitamin B12 which were higher in the chitosan NPs loaded with BVE than BVE alone. Furthermore, *C. auris* recorded the highest value in minimum inhibitory concentration and sub-minimum inhibitory concentration of chitosan NPs loaded BVE 52.3 and 39.23, respectively.

Conclusion: The prepared NPs compound was exceeded on BVE alone and highly sensitive antibiotic as anticandidal and antibiofilm activity against extremely drug-resistant *Candida* spp., including *C. auris*.

Keywords: Chitosan nanoparticles (CSNPs), *Beta vulgaris* L., Extensively drug-resistant (XDR), *Candida*, *Candida auris*, Antifungal, Antibiofilm

Introduction

Nanotechnology is a field of applied science that studies materials on a scale between 1-100 nm. Recently, it has submitted submissions in biology, electronics, and medicine abroad. The extended development of nanotechnology and its science led to the motivation to develop industries (Hejazy & Koohi, 2017; Zahin et al., 2020). The small size of nanoparticles (NPs) means that they can easily enter the body and cross a variety of biological obstructions to reach the most vulnerable organs (Kaboutari et al., 2023; Othman et al., 2020). A wide range of plants are cultivated globally for food and medicinal purposes, with several traditional medicinal plants displaying significant potential in the management and treatment of various modern health problems. These include beetroot (*Beta vulgaris* L. extract [BVE]), known in the Middle East as Shamandar, a plant of the family Amaranthaceae (Albasher et al., 2020). *B. vulgaris* L. contains two major betalain pigments, red betanin, and yellow violaxanthin I, which have been considered for a long time as the unique source of betalains. Red beet is cultivated all over the world and is commonly and frequently consumed. The world production of beetroot was estimated to be about 275 million metric tons in 2018 (Fu et al., 2020). Betacyanins constitute approximately 75% to 95% of beetroot pigments, and the remaining 5% to 25% are betaxanthins (Sadowska-Bartosz & Bartosz, 2021). Fungal infections caused by *Candida* species and the increasing prevalence of Azole-resistant strains in immunocompromised patients are critical (Fetouh et al., 2023; Habib et al., 2007; Shokri et al., 2016). Recently, in addition to trying to make effective chemical treatments and probiotic therapy for the treatment of candidiasis, many metal NPs have been studied in the treatment of this disease and have received significant results (Yousefi et al., 2019). NPs prepared with chitosan and derivatives of these NPs typically possess a positive surface charge and mucoadhesive properties, such that can adhere to mucus membranes and release the drug payload in a sustained release manner. Chitosan-based NP has various applications in NPs as antimicrobial drugs (Al Sahib & Awad, 2022). Among the new antimicrobial agents, special attention has been paid to NPs. NPs have a higher level than other antifungal agents, and in addition, they have a better penetration in tissues and cells (Kumar & Anthony, 2016).

Materials and Methods

Microorganisms in the study

Candida spp. including (*C. parapsilosis*, *C. glabrata*, *C. lusitaniae*, and *C. auris*) were isolated from different clinical sources and identified using the CHROMagar *Candida* culture medium (*C. auris* is not included in this medium), ViteK-2 system, and molecular diagnostics. The isolates were obtained from the College of Science for Women laboratories.

Biofilm formation test

For the study of biofilm formation, the microtiter plate assay for studying biofilm formation is a method that allows for the observation of *Candida* adherence to an abiotic surface. In this assay, *Candida* was incubated in vinyl "u"-bottom or other types of 96-well microtiter plates. Following incubation, planktonic yeast is rinsed away, and the remaining adherent *Candida* (biofilms) are stained with crystal violet dye, thus allowing visualization of the biofilm. If quantitation is desired, the stained biofilms are solubilized and transferred to a 96-well optically clear flat-bottom plate for measurement by spectrophotometry.

Preparation of *Beta vulgaris* L. extract

The BV was purchased from a local market in Baghdad, Iraq, and identified at the herbarium in the Department of Biology, College of Science, University of Baghdad. Aqueous and ethanol extracts of the *B. vulgaris* L. were prepared according to (Sultana et al., 2009). The air-dried beetroot (150 g) was extracted using aqueous methanol (500 mL) as a solvent (methanol: water, 80% V/V) for 8 h, in the Soxhlet apparatus. The extract was concentrated using a rotary evaporator and then the remained extracts were dried. The extract yield was calculated by the dried concentrated crude extracts.

Biosynthesis of chitosan NPs loaded BVE

Chitosan 5% (200 mg of CS +100 mL acetic acid) and BVE 1% (1 g of BVE + 100 mL distal water) were combined in equimolar ratios, and the condensation process was carried out in the presence of xylene using the Dean-Stark (Clevenger) apparatus until the theoretical quantity of water was separated. Chitosan amide product was separated by filtration, washed several times with methanol, hot distilled water, and ethanol, and then dried in an electric oven at 50 ˚C and weighed (Abd El-Ghaffar & Hashem, 2010).

Characterization (morphological and structural aspects) of chitosan NPs loaded BVE

Various approaches were used to characterize to identify chitosan NPs (CSNPs) loaded BVE in this study, namely, ultraviolet-visible absorption spectroscopy (Agarwal et al., 2018)., atomic force microscopy (AFM) (Du et al., 2008)., scanning electron microscopy (SEM) analysis (Atangana et al., 2019)., x-ray diffraction (XRD) (Anand et al., 2018)., energy dispersive x-ray (EDX) (Hodoroaba, 2020)., and high-performance liquid chromatography (HPLC) analysis for the determination of phenolic compounds (Dahl-Lassen et al., 2018).

Determination of minimum inhibitory concentration and sub-minimum inhibitory concentration

Spread plate method (SPM)

The spread plate method (SPM method is used as described by Wise, 2006. Sabouraud dextrose agar is put onto several sterile petri plates and allowed to solidify. Before using the plates, we must wait for a while to dry. As with the pour plate procedure, *Candida* suspension of moderate turbidity was prepared by picking 1-2 isolated colonies of candida from the original culture and introducing them into a test tube containing 4 mL of normal saline. It was compared to the standard turbidity solution 0.5 McFarland which approximately equals 1.5×10^8 colony-forming unit/milliliters (CFU/mL). The treatments were with different concentrations, namely 50%, 25%, 12.5%, 6.25%, and 3.12% of CSNPs loaded BVE solution mix with *Candida* suspension, in addition to *Candida* control (without treatment), pipetted with 100 µL quantities of each dilution over the surface of each of the three plates. An ethanol-flamed glass spreader was then used to disseminate the sample throughout the plate's surface. The plates were then incubated for 24 h at 37 ˚C in aerobic conditions and the number of colonies that form is counted in the same way as the pour plate method.

Determination of inhibition efficacy against biofilm production

The microtiter plate assay is a qualitative technique that uses a microplate reader to determine an agent's effectiveness against biofilm formation. The sub-minimum inhibition concentrations (sub-MIC) obtained from the previous experiment were used to study the effect of the test materials on the formation or inhibition of biofilm of the studied *Candida* spp. isolates that produce strong biofilm. The test materials were BVE, CSNPs loaded BVE solution, positive control (*Candida* suspension only), and negative control (brain heart infusion broth [BHIB] only). However, 100 µL of test compounds was added and the plate was incubated at 37 ˚C for 24 h. After that, all wells were washed, stained, and read at 600 nm wavelength using a microplate reader percent of biofilm inhibition was calculated by equation (Shinde et al., 2021).

Results and Discussion

Detection of the fungal ability for biofilm formation

In this study, the determination of the ability of *Candida* spp. isolates for adherence and producing a slime layer (biofilm formation) was experienced by using a microtiter plate and read by a microplate spectrophotometer as in (Figure 2). We noticed that all isolates produced biofilm in varying proportions.

Our study's findings are in line with the results of Marak and Dhanashree, (2018). Meanwhile, *C. albicans* (45.5%) was the most prevalent species among the 90 *Candida* spp. that were isolated, followed by *C. tropicalis* (28.88%), *C. krusei* (20%), *C. glabrata* (3.33%), and *C. parasilosis* (2.22%). Also, *Candida* spp. was found

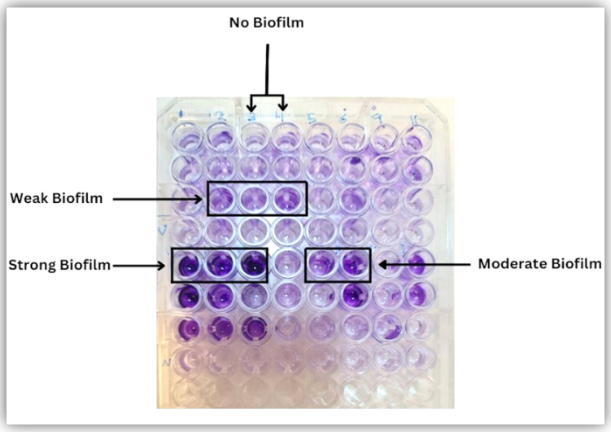

Figure 1. Microtiter plate assay of biofilm formation

in the following samples: Pus, bile aspirate, deep tissue, high vaginal swabs, suction tips, blood, wound swabs, and urine.

Biosynthesis of chitosan NPs loaded BVE

Chitosan and BVE adduct were prepared and then the tripolyphosphate (TPP) was added to form CSNPs loaded BVE. When chitosan reacts with TPP, the amine groups of the chitosan can cross-link with the phosphine groups of TPP to create NPs. During the action, the chitosan's molecular structure will be altered, resulting in a change in solubility in an acid solution as well as a gel-like solution or a liquid form (Kahdestani et al., 2021). The appearance of a clear color indicates the formation of NPs loaded with the plant extract as shown in Figure 1.

Characterization of chitosan NPs loaded BVE

The CSNPs loaded BVE were characterized by employing ultraviolet-visible spectroscopy, SEM, EDX, AFM, and XRD, analyses through examining the morphological, structural, and optical properties as shown below.

Ultraviolet-visible spectroscopy

Ultraviolet-visible spectroscopy is a primary step in confirmation of the synthesis of CSNPs loaded BVE. The absorbances of BVE and CSNPs loaded BVE were measured and the results are shown in Figure 2 for BVE and CSNPs loaded BVE as shown in Figure 3. In the CSNPs loaded BVE, the highest absorbance value was 0.087, while the lowest absorbance value was 0.006 at wavelengths 279 nm and 542 nm, respectively. On the other hand, for BVE the highest absorbance value was 3.135 and the lowest absorbance value was 1.063 at

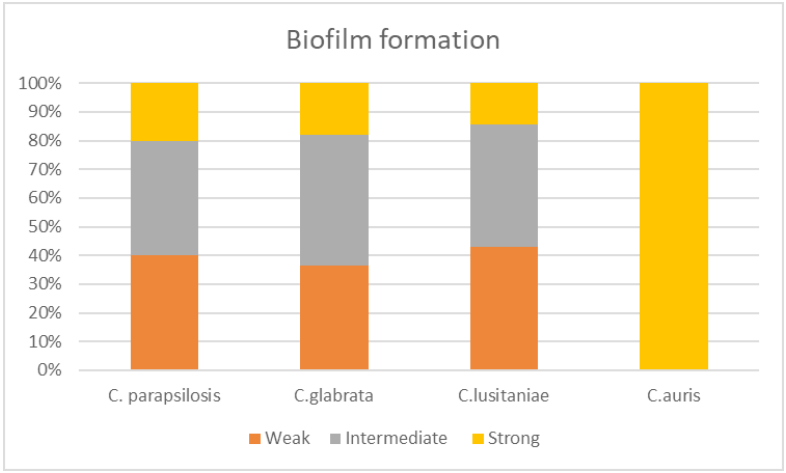

Figure 2. Biofilm formation of *Candida* spp.

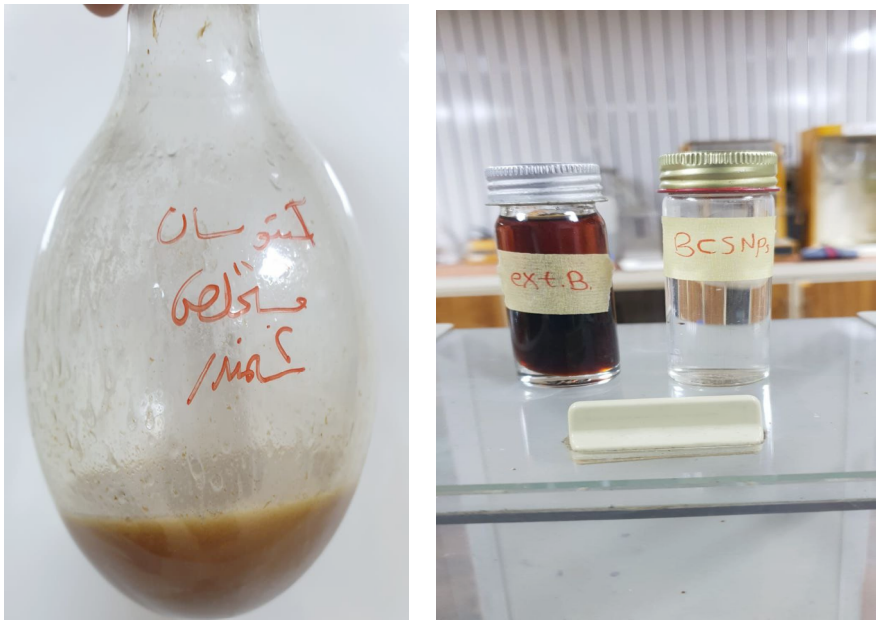

Figure 3. Formation of NPs loaded with the plant extract (chitosan NPs loaded BVE)

wavelengths 212 nm, and 282 nm, respectively. However, for chitosan the absorbance value was 2.85 at wavelengths 212 nm, The decrease in the absorbance value at wavelength 282 nm in the BVE to 212 nm in CSNPs loaded BVE, as well as the highest absorbance value at the wavelength 254 nm with a value of 0.006 in CSNPs loaded BVE material after it was the highest value in BVE at a wavelength of 282 nm with a value of 1.063, in addition to the disappearance of the wavelength 282 nm in the BVE and the appearance of a new wavelength with high absorbance at 542.00 in CSNPs loaded BVE all, indicate the formation of the nanomaterial and the successful loading of the BVE on chitosan NPs.

XRD

The XRD patterns of chitosan show the main peak of 2θ value at 20.53° and an intensity level close to 1200 count; on the other hand, as shown in Figure 4, the CSNPs loaded BVE peak, which shows its main peak of 2θ value at 22.8596° and an intensity level at 736.5503 count, this change indicates the difference in the crystal structure between these two materials were CSNPs loaded BVE was more crystalline than CS, as well as the CS diffraction peak, which was previously found at 20.53, has shifted to a higher value 22.8596° in this study, which may be related to the interaction of CS loaded with BVE to form CSNPs loaded BVE.

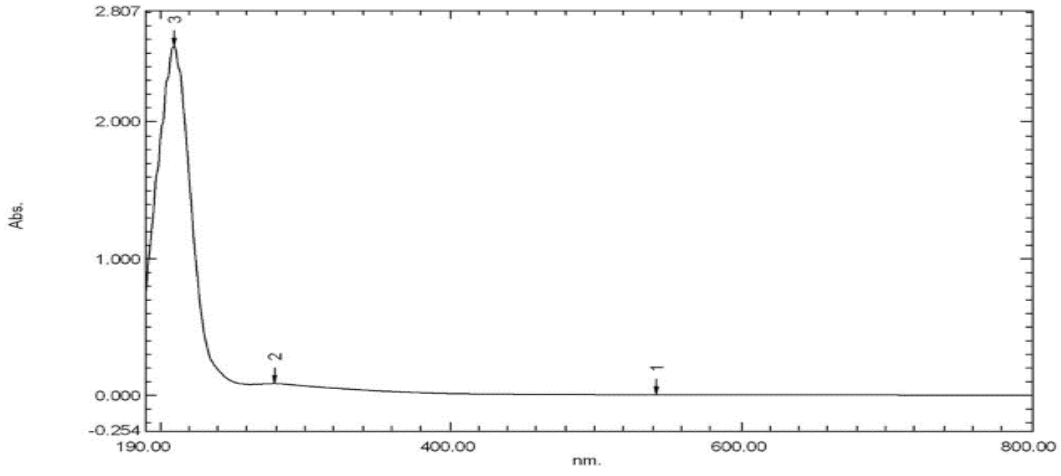

Figure 4. Ultraviolet-visible spectroscopy analysis for chitosan NPs loaded BVE

Table 1. Ultraviolet-visible spectral analysis results of chitosan NPs loaded BVE

Peak No.	Wavelength (nm)	Absorbance
1	542	0.006
2	279	0.087
3	210	2.552

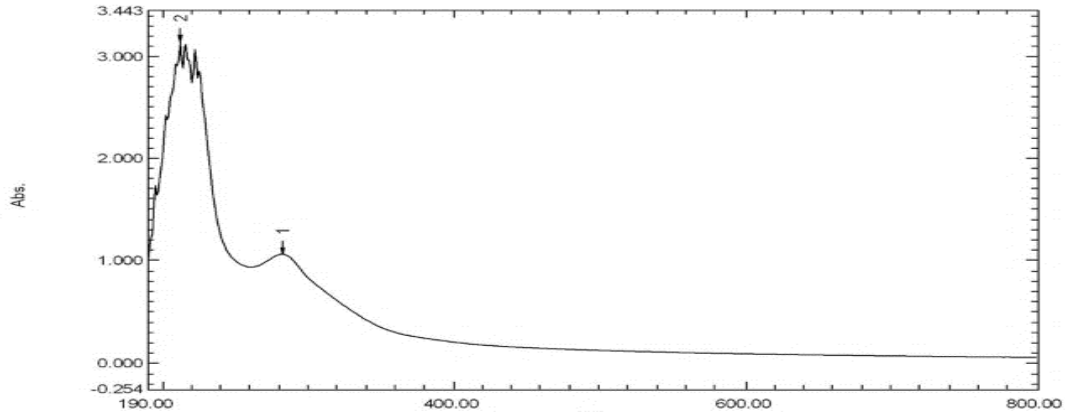

Figure 5. Ultraviolet-visible spectroscopy analysis for BVE

The XRD results suggested that the particle size effects are generally responsible for the widening of peaks in crystalline XRD patterns. Wider peaks indicate lower particle sizes and reflect the influence of experimental circumstances on particle structures. Small crystals have a limited number of levels of reflection with low intensity, while large crystals have a large number of these levels with high intensity; therefore, XRD peaks are formed due to reflection from crystal levels and the decrease in intensity is visible in the pattern of CSNPs loaded BVE, which exhibits suppressed peaks (Table 1).

These results were in line with the study of Anand et al. (Anand et al., 2018) who found the pure chitosan diffraction peak, which was previously found at 20.20 ˚C, has migrated to a lower value 19.85 ˚C, which may be attributed to the interaction of CSNPs with TPP and the crystalline structure of CSNPs. Kahdestani et al. (2021) found that the variations among the patterns might be traced to molecular arrangement changes in the crystal lattice, and the pattern of teicoplanin-loaded chitosan NPs displays reduced peaks at 2θ 22 ˚C and 25 ˚C, indicating an intensity decrease.

Atomic force microscopy

AFM images were used to measure particle size and the topography of the surface of CSNPs loaded BVE, the particle size ranged from 26.74 to 53.96 nm, and the 3D image of CSNPs loaded BVE revealed a population of homogeneous particles with a regular surface shape (Figures 5 and 6).

The images of AFM demonstrated smart interaction among CSNPs loaded BVE, leading to the formation of well discrete aggregates, From the information included with the image, the evolution values of root mean square, surface roughness average, and average grain size were calculated and listed that exhibited information about coverage area minimum, maximum, and mean particle size. These results are in line with Zheng et al., 2021 who found that the resulting morphological-mediated chito-

Table 2. Ultraviolet-visible spectral analysis results of BVE

Peak No.	Wavelength (nm)	Absorbance
1	282	1.063
2	212	3.135

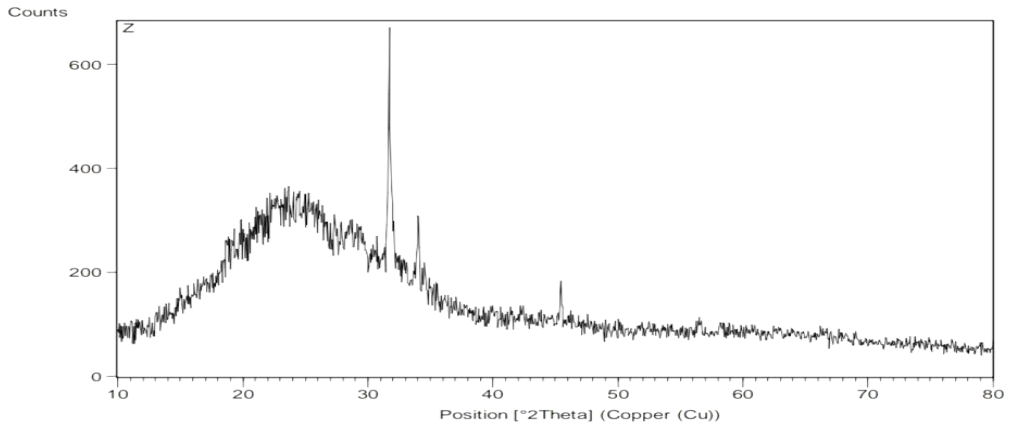

Figure 6. XRD of chitosan NPs loaded BVE

san was exhibited with uniform particles, and their average size was 40–96 nm.

Scanning electron microscope

The morphology of CSNPs loaded BVE was investigated using a scanning electron microscope (SEM), the result was presented in Figure 7, CSNPs loaded BVE has a spherical appearance with a diameter range of 37.99-56.28 nm, and have a relatively homogeneous morphology, the larger particles may be a result of the unwanted aggregation that occurs throughout the drying process (Table 2). Agglomeration occurs as soon as the liquid evaporates leading to rising particle concentration. The increase in dissolved ion concentration caused by liquid evaporation can reduce the electrostatic repulsive force, facilitating agglomeration (Shrestha et al., 2020).

Energy dispersive x-ray

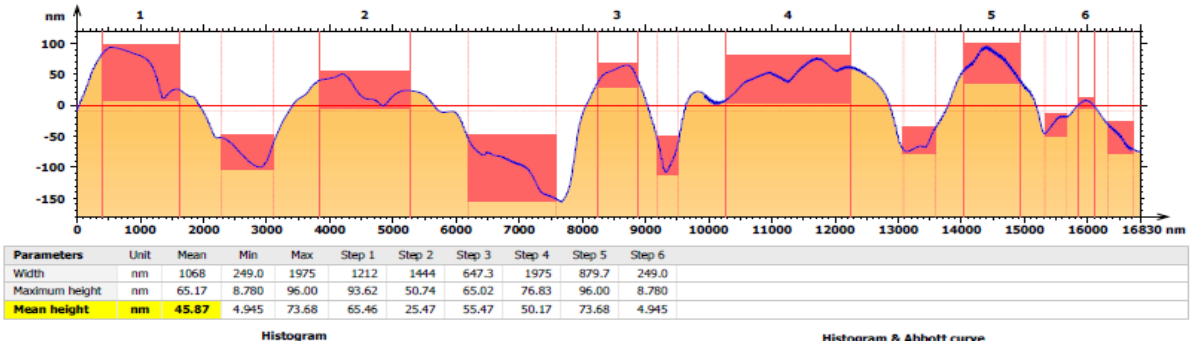

Parameters	Unit	Mean	Min	Max	Step 1	Step 2	Step 3	Step 4	Step 5	Step 6
Width	nm	1068	249.0	1975	1212	1444	647.3	1975	879.7	249.0
Maximum height	nm	65.17	8.780	96.00	93.62	50.74	65.02	76.83	96.00	8.780
Mean height	**nm**	**45.87**	4.945	73.68	65.46	25.47	55.47	50.17	73.68	4.945

Figure 7. The particles size of chitosan NPs loaded BVE

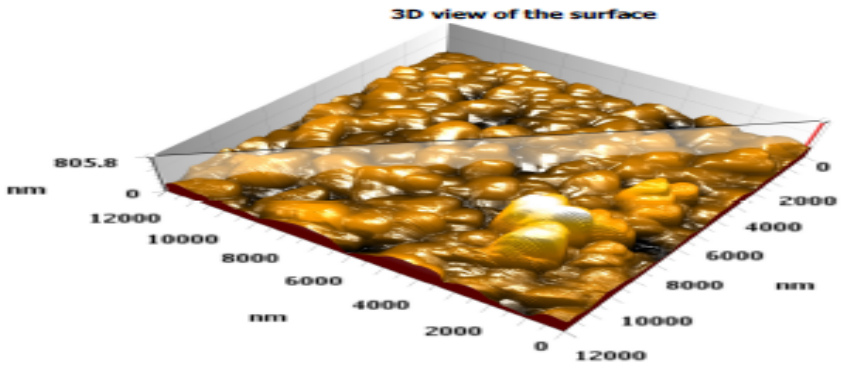

Figure 8. 3D Image of chitosan NPs loaded BVE

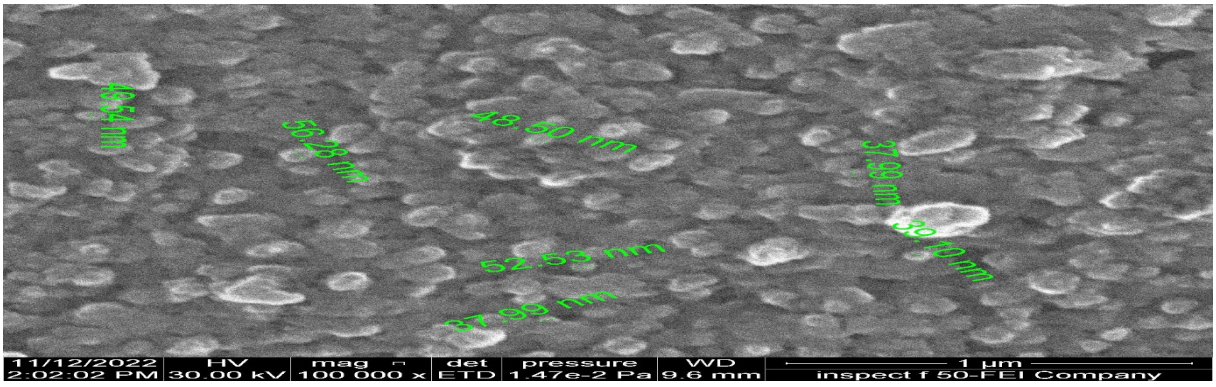

Figure 9. Scanning electron microscopy image of chitosan NPs loaded BVE

The elemental analysis of CSNPs loaded BVE via SEM-EDX revealed the presence of C, O, Mg, Na, and Ca. Figure 8 shows that EDX examination reveals a significant signal at 1.5 keV and 2.3 keV due to the presence of carbon and oxygen respectively, confirming the presence of chitosan. The other elements, such as Ca and Mg are due to the presence of BVE components. The results are in line with Raza and Anwar (Raza & Anwar, 2017) who used scanning electron microscopy equipped with EDX to confirm the presence of CSNPs on the treated fabric. Also, Omidi and Kakanejadifard (Omidi & Kakanejadifard, 2019) reported that the EDX spectrum of CS10 contains four kinds of elements C, O, N, and Br. Also, CSNP10 consists of C, O, N, P, and Br elements.

Quantification of bioactive compounds by high-performance liquid chromatography (HPLC) mass spectrometry/mass spectrometry system

The chromatographic analysis of BVE showed the existence of flavonoids (ferulic acid, quercetin, and rutin), phenols (caffeic acid, gallic acid, and chlorogenic acid), lysine, and vitamin B12; however those were higher in the nano sample than the extracted sample and the highest concentration recorded in caffeic acid in nano sample was 865.5 parts per million as shown in Table 3.

The detection results of active compounds in the extract proved that it contained most of these compounds in good proportions, which are responsible for the biological activity of medicinal plants which indicates that the BVE possesses a good therapeutic property according to the function of each group.

Determination of the minimum inhibition concentration (MIC)

There were differences in MIC and sub-MIC of CSNPs loaded BVE and only BVE against the isolates; however, *C. auris* recorded the highest value in CSNPs loaded BVE which MIC of CSNPs loaded BVE was 52.3 and sub-MIC was 39.23 while the other isolates showed same MIC and Sub-MIC of CSNPs loaded BVE and only BVE as shown in Figure 9.

The findings are in line with Lin et al., 2023, who showed that berberine-loaded chitosan NPs released from berberine (BBR)-CSNPs could inhibit the growth of *C. albicans* and destroy the integrity of the cell wall and cell membrane of *C. albicans*.

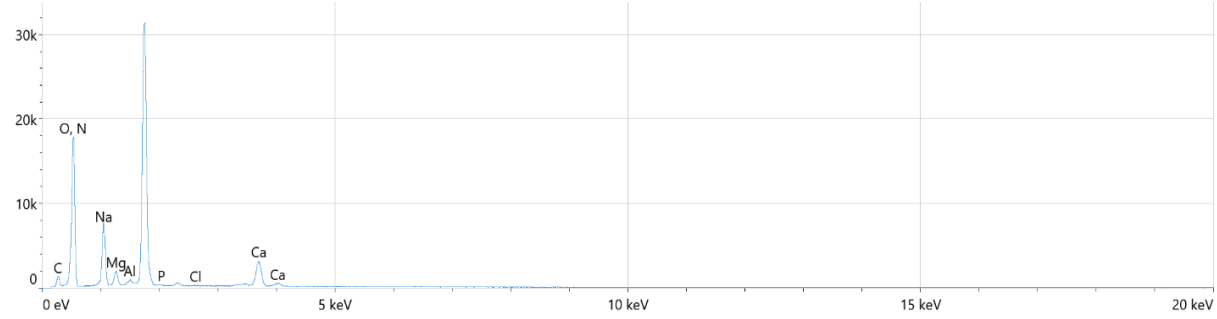

Figure 10. Spectrum of elemental analysis of chitosan NPs loaded BVE by energy dispersive x-ray

Table 3. The chromatographic analysis of chitosan NPs loaded BVE

Components	Extract Sample	Nano Sample
Caffeic acid (ppm)	541	231.2
Gallic acid (ppm)	2.751	865.5
Chlorogenic acid (ppm)	4.215	1.767
Qurcetine (ppm)	4.367	1.853
Ferulic acid (ppm)	4,062	2.385
Rutin (ppm)	1.555	465.4
Vitamin B 12 (ppm)	4.967	2.836
Lysin (ppm)	10.862	5.308

Ppm: Parts per million.

Estimation of antibiofilm activity of chitosan NPs loaded BVE

The inhibition rate of CSNPs loaded BVE was higher in 1:5 than in 1:4; however, the antibiofilm activity showed less against *C. auris* compared to other isolates as shown in Figure 10.

The findings are in line with Lin et al., 2023. that showed berberine-loaded chitosan NPs (the free BBR and BBR-CSNPs) had a significant inhibitory effect on *C. albicans* biofilm, and the inhibitory effect on biofilm was concentration-dependent. Free BBR even at the lowest concentration (64 µg/mL), about 40% of the *C. albicans* biofilm formation was inhibited. When free BBR concentration was higher than 512 µg/mL, almost no biofilm formation was observed. In the same

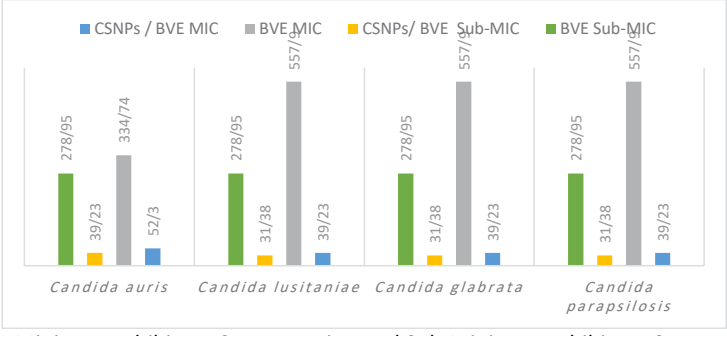

Figure 11. Minimum inhibitory concentration and sub-minimum inhibitory concentration of chitosan NPs loaded BVE and BVE against *Candida* spp.

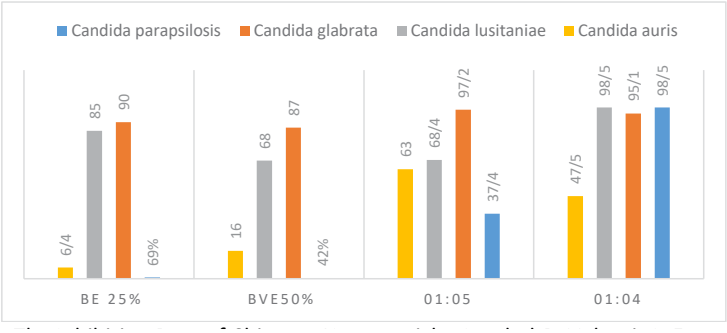

Figure 12. The inhibition rate of chitosan NPs loaded BVE against *Candida* spp.

concentration range, BBR-CSNPs showed lower inhibitory activity on the biofilm of *C. albicans* compared with free BBR. Also, the results are in line with Tan et al., 2022 who found that CSNPs loaded with amphotericin B inhibited planktonic cell growth and biofilm formation effectively and exhibited the highest efficacy on the removal of a mature biofilm than free amphotericin B or CSNPs- amphotericin B On *Candida* biofilm-related infections.

The nanostructures and positive charge of CSNPs make them have good permeability and easy to combine with the cells on the surface and inside the biofilm, causing the change of cell surface charge, increasing the sensitivity of cells to drugs, and then affecting the formation of biofilm (Li et al., 2021). Moreover, the nanostructure and positive charge of BBR-CSNPs had good permeability and were easy to combine with microbial cells. Secondly, CS can also form NPs with polyanion TPP through electrostatic interaction in an aqueous solution. CSNPs have small particle sizes and large specific surface area (Tan et al., 2022). The results also indicated that CSNPs loaded BVE was easier to penetrate the biofilm and kill the cells in the biofilm of *Candida* spp.

CSNP prepared using low molecular weight and high molecular weight of chitosan have been evaluated for their antifungal activity against *C. albicans*, *Fusarium solani*, and *Aspergillus niger*. The NPs prepared with different concentrations of chitosan showed an inhibitory effect against the three fungal species. While A. niger exhibited a strong resistance to CNPs which was fabricated with low concentrations of chitosan (Ing et al., 2012). The CSNPs were also evaluated as a controlling agent for various plant diseases caused by *Rhizoctonia solani*, *Fusarium oxysporum*, *Collectotrichum acutatum*, and *Phytophthora infestans*.

Moreover, CNP shave has been shown as an ideal coating agent for coated vegetables by improving the shelf life of tomato, chilly, and brinjal. CSNPs exhibited significant antifungal activity against all fungal species. Vegetable samples treated with different concentrations that ranged from 1% to 5% of CSNPs prevented weight loss compared to uncoated vegetable samples (Divya et al., 2018).

Conclusion

The prepared NPS compound was exceeded on BVE alone and highly sensitive antibiotic as antifungal and antibiofilm activity against extensively drug-resistant (XDR) *Candida* spp. including *C. auris* isolate. CSNPs loaded BVE showed antibiofilm activity more than BVE against some resistance *Candida* spp.

Ethical Considerations

Compliance with ethical guidelines

The research did not involve any ethical considerations.

Funding

This research did not receive any grant from funding agencies in the public, commercial, or non-profit sectors.

Authors' contributions

All authors contributed equally to the conception and design of the study, data collection and analysis, interpretation of the results, and drafting of the manuscript. Each author approved the final version of the manuscript for submission.

Conflict of interest

The authors declared no conflict of interest.

Acknowledgments

The authors would like to express their sincere gratitude to all those who contributed to the successful completion of this research.

References

Abd El-Ghaffar, M. A., & Hashem, M. S. (2010). Chitosan and its amino acids condensation adducts as reactive natural polymer supports for cellulase immobilization. *Carbohydrate Polymers, 81*(3), 507-516. [DOI:10.1016/j.carbpol.2010.02.025]

Agarwal, M., Agarwal, M. K., Shrivastav, N., Pandey, S., Das, R., & Gaur, P. (2018). Preparation of chitosan nanoparticles and their in-vitro characterization. *International Journal of Life-Sciences Scientific Research, 4*(2), 1713-1720. [Link]

Al Sahib, S. A., & Awad, S. H. (2022). Synthesis, characterization of chitosan para- hydroxyl benzaldehyde schiff base linked maleic anhydride and the evaluation of its antimicrobial activities. *Baghdad Science Journal, 19*(6), 1265-1275. [DOI:10.21123/bsj.2022.5655]

Albasher, G., Albrahim, T., Alsultan, N., Alfaraj, S., Alharthi, M. S., & Kassab, R. B., et al. (2020). Red beetroot extract mitigates chlorpyrifos-induced nephrotoxicity associated with oxidative stress, inflammation, and apoptosis in rats. *Environmental*

Science and Pollution Research International, 27(4), 3979–3991. [DOI:1007/s11356-019-07009-6] [PMID]

Anand, M., Sathyapriya, P., Maruthupandy, M., & Beevi, A. H. (2018). Synthesis of chitosan nanoparticles by TPP and their potential mosquito larvicidal application. *Frontiers in Laboratory Medicine, 2*(2), 72-78. [DOI:10.1016/j.flm.2018.07.003]

Atangana, E., Chiweshe, T. T., & Roberts, H. (2019). Modification of novel chitosan-starch cross-linked derivatives polymers: Synthesis and characterization. *Journal of Polymers and the Environment, 27,* 979-995. [DOI:10.1007/s10924-019-01407-0]

Dahl-Lassen, R., van Hecke, J., Jørgensen, H., Bukh, C., Andersen, B., & Schjoerring, J. K. (2018). High-throughput analysis of amino acids in plant materials by single quadrupole mass spectrometry. *Plant Methods, 14,* 8. [DOI:10.1186/s13007-018-0277-8] [PMID]

Divya, K., Smitha, V., & Jisha, M. S. (2018). Antifungal, antioxidant and cytotoxic activities of chitosan nanoparticles and its use as an edible coating on vegetables. *International Journal of Biological Macromolecules, 114,* 572-577. [DOI:10.1016/j.ijbiomac.2018.03.130] [PMID]

Du, W. L., Xu, Z. R., Han, X. Y., Xu, Y. L., & Miao, Z. G. (2008). Preparation, characterization and adsorption properties of chitosan nanoparticles for eosin Y as a model anionic dye. *Journal of Hazardous Materials, 153*(1-2), 152-156. [DOI:10.1016/j.jhazmat.2007.08.040] [PMID]

Fetouh, M., Elbarbary, H., Ibrahim, E., & Maarouf, A. A. (2023). Effect of adding lactoferrin on some foodborne pathogens in yogurt. *Iranian Journal of Veterinary Medicine, 17*(3), 189-198 [DOI:10.32598/IJVM.17.3.1005313]

Fu, Y., Shi, J., Xie, S. Y., Zhang, T. Y., Soladoye, O. P., & Aluko, R. E. (2020). Red beetroot betalains: Perspectives on extraction, processing, and potential health benefits. *Journal of Agricultural and Food Chemistry, 68*(42), 11595-11611. [DOI:10.1021/acs.jafc.0c04241] [PMID]

Habib, K., Latif, H. A., & Jassim, A. N. (2007). Study a bout the Epidemiology of Vulvo Vaginal Candidiasis (Candida spp.) in Baghdad City. *Baghdad Science Journal, 4*(1), 1-6. [DOI:10.21123/bsj.4.1.1-6]

Hejazy, M., & Koohi, M. K. (2017). Effect of subacute exposure of nano Zinc particles on oxidative stress parameters in rats. *Iranian Journal of Veterinary Medicine, 11*(2), 155-164. [DOI:10.22059/ijvm.2017.61936]

Hodoroaba, V. D. (2020). Energy-dispersive X-ray spectroscopy (EDS). In V. D. Hodoroaba, W. Unger, & A. G. Shard (Eds.), *Characterization of nanoparticles* (pp. 397-417). Amsterdam: Elsevier. [DOI:10.1016/B978-0-12-814182-3.00021-3]

Ing, L. Y., Zin, N. M., Sarwar, A., & Katas, H. (2012). Antifungal activity of chitosan nanoparticles and correlation with their physical properties. *International Journal of Biomaterials, 2012*(1), 632698. [DOI:10.1155/2012/632698]

Kaboutari, J., Ghorbani, M., Karimibabaahmadi, B., Javdani, M., & Khosraviyan, P. (2023). Anti-inflammatory evaluation of the novel slow-release curcumin-loaded selenium nanoparticles in the experimental peritonitis. *Iranian Journal of Veterinary Medicine*.

Kahdestani, S. A., Shahriari, M. H., & Abdouss, M. (2021). Synthesis and characterization of chitosan nanoparticles containing teicoplanin using sol-gel. *Polymer Bulletin, 78*(2), 1133-1148. [DOI:10.1007/s00289-020-03134-2]

Kumar, V. V., & Anthony, S. P. (2016). Antimicrobial studies of metal and metal oxide nanoparticles. In A. M. Grumezescu (Ed.), *Surface chemistry of nanobiomaterials* (pp. 265-300). Amsterdam: Elsevier. [DOI:10.1016/B978-0-323-42861-3.00009-1]

Li, X., Chen, D., & Xie, S. (2021). Current progress and prospects of organic nanoparticles against bacterial biofilm. *Advances in Colloid and Interface Science, 294,* 102475. [DOI:10.1016/j.cis.2021.102475] [PMID]

Lin, Q., Li, Y., Sheng, M., Xu, J., Xu, X., & Lee, J., et al. (2023). Antibiofilm effects of berberine-loaded chitosan nanoparticles against Candida albicans biofilm. *LWT, 173,* 114237. [DOI:10.1016/j.lwt.2022.114237]

Marak, M. B., & Dhanashree, B. (2018). Antifungal susceptibility and biofilm production of Candida spp. Isolated from clinical samples. *International Journal of Microbiology, 2018,* 7495218. [DOI:10.1155/2018/7495218] [PMID]

Omidi, S., & Kakanejadifard, A. (2019). Modification of chitosan and chitosan nanoparticle by long chain pyridinium compounds: Synthesis, characterization, antibacterial, and antioxidant activities. *Carbohydrate Polymers, 208,* 477-485. [DOI:10.1016/j.carbpol.2018.12.097] [PMID]

Othman, M. S., Hafez, M. M., & Abdel Moneim, A. E. (2020). The potential role of zinc oxide nanoparticles in MicroRNAs dysregulation in STZ-induced type 2 diabetes in rats. *Biological Trace Element Research, 197*(2), 606-618. [DOI:10.1007/s12011-019-02012-x] [PMID]

Raza, Z. A., & Anwar, F. (2017). Fabrication of chitosan nanoparticles and multi-response optimization in their application on cotton fabric by using a Taguchi approach. *Nano-Structures & Nano-Objects, 10,* 80-90. [DOI:10.1016/j.nanoso.2017.03.007]

Sadowska-Bartosz, I., & Bartosz, G. (2021). Biological properties and applications of betalains. *Molecules, 26*(9), 2520. [DOI:10.3390/molecules26092520] [PMID]

Shinde, S., Lee, L. H., & Chu, T. (2021). Inhibition of biofilm formation by the synergistic action of EGCG-S and antibiotics. *Antibiotics, 10*(2), 102. [DOI:10.3390%2Fantibiotics10020102] [PMID]

Shokri, H., Sharifzadeh, A., & Khosravi, A. (2016). Antifungal activity of the Trachyspermum ammi essential oil on some of the most common fungal pathogens in animals. *Iranian Journal of Veterinary Medicine, 10*(3), 173-180. [DOI:10.22059/ijvm.2016.58679]

Shrestha, S., Wang, B., & Dutta, P. (2020). Nanoparticle processing: Understanding and controlling aggregation. *Advances in Colloid and Interface Science, 279,* 102162. [DOI:10.1016/j.cis.2020.102162] [PMID]

Sultana, B., Anwar, F., & Ashraf, M. (2009). Effect of extraction solvent/technique on the antioxidant activity of selected medicinal plant extracts. *Molecules, 14*(6), 2167-2180. [DOI:10.3390/molecules14062167] [PMID]

Tan, Y., Ma, S., Ding, T., Ludwig, R., Lee, J., & Xu, J. (2022). Enhancing the antibiofilm activity of β-1, 3-glucanase-functionalized nanoparticles loaded with amphotericin B against *Candida albicans* biofilm. *Frontiers in Microbiology, 13,* 815091. [DOI:10.3389/fmicb.2022.815091] [PMID]

Wise, K. (2006). Preparing spread plates protocols. *American Society for Microbiology*, 1-8. [Link]

Yousefi, B., Eslami, M., Ghasemian, A., Kokhaei, P., & Sadeghnejhad, A. (2019). Probiotics can really cure an autoimmune disease? *Gene Reports, 15,* 100364. [DOI:10.1016/j.genrep.2019.100364]

Zahin, N., Anwar, R., Tewari, D., Kabir, M. T., Sajid, A., & Mathew, B., et al. (2020). Nanoparticles and its biomedical applications in health and diseases: Special focus on drug delivery. *Environmental Science and Pollution Research, 27*(16), 19151-19168. [DOI:10.1007/s11356-019-05211-0] [PMID]

Zheng, S., Bawazir, M., Dhall, A., Kim, H. E., He, L., & Heo, J., et al. (2021). Implication of surface properties, bacterial motility, and hydrodynamic conditions on bacterial surface sensing and their initial adhesion. *Frontiers in Bioengineering and Biotechnology, 9,* 643722. [DOI:10.3389/fbioe.2021.643722] [PMID]